WESTWARD TRAVELING S DYNAMICS AND THE LOCAL STRUCTURE OF AN ISOLATED SUBSTORM

L. Lazutin[1,2], G. Starkov[2], C-I. Meng[3], D. G. Sibeck[3], J. Stadsnes[4], J. Bjordal[4], Kan Liou[3], T. Kornilova[2], and G. Reeves[5]

[1]Space Physics Division, Skobeltsyn Institute of Nuclear Physics, Moscow State University, Moscow, 119899, Russia, [2]Polar Geophysical Institute, Apatity, Murmansk Region, 184200, Russia, [3]Applied Physics Laboratory, Johns Hopkins University, Laurel, MD 20723, USA, [4]Department of Physics, University of Bergen, Bergen, N-5007, Norway, [5]Los Alamos National Laboratory, Los Alamos, NM 87545, USA

ABSTRACT

We present a case study of a simple isolated substorm. We compare magnetic field and optical observations at Kola Peninsula with POLAR UVI, POLAR/PIXIE and LANL satellite data to examine the relationshipships between global and local auroral structures and their dynamics. In addition to the active phase of the substorm with a main onset, there are two additional Westward Traveling Surge (WTS) intensifications accompanied by energetic particle acceleration and magnetic field dipolarization in associated local sectors of the magnetosphere. The longitudinal dimensions of the main auroral bulge and the WTS were restricted and in neighboring sectors quite different types of the activity were observed. The effects of the fragmentation of the night side auroral magnetosphere into sectors with simultaneous auroral bulge expansion and the local growth phase may help explain the temporal structure of multiple-onset substorms. Related problems of the substorm geometry are briefly discussed.

INTRODUCTION

This paper presents a substorm case study which differs from other case studies by its emphasis on the relationships between local and global substorm dynamics deduced from simultaneous auroral observations from the ground and satellite. Ground-based magnetometers and auroral TV records provide the local view. The global auroral oval structure is monitored with the help of POLAR ultraviolet (UVI) and X-ray (PIXIE) observations reflecting the low- and high-energy auroral particle precipitation. IMP-8 provided solar wind observations while LANL geosynchronous spacecraft provided energetic particle observations that prove important in identifying key points of the substorm development.

Case studies usually allow us to consider several aspects of the magnetosphere substorm physics. We will briefly discuss longstanding problem of the substorm geometry, and reach a conclusion favoring the inner magnetosphere onset models and the problem of the substorm triggering, which is also under continuing discussion (e.g., Sharma and Baker, (1998) and other reports in the same Substorm-4 session). However, most of our attention will be devoted to the temporal structure of the substorm, spatial localization of the substorm modules and interrelationships between the processes in different local sectors.

Substorm models and numerical simulations are usually based on oversimplified substorm schematics, particularly during the active phase, which is regarded as a simple auroral bulge expansion. Of cause, substorms may have multiple intensifications (Rostoker et al, 1980), and there are numerous publications on the fine spatial and temporal structure seen during substorms (e.g., Elphinstone, 1996). The importance of these local details of the substorm in understanding substorm physics is not commonly accepted, and a single-step global expansion scenario prevails.

Nevertheless, "classical" isolated substorms are the exception rather than the rule. The simplest isolated substorm during the 1998-1999 winter season for which ground-based TV and POLAR UVI and PIXIE data were

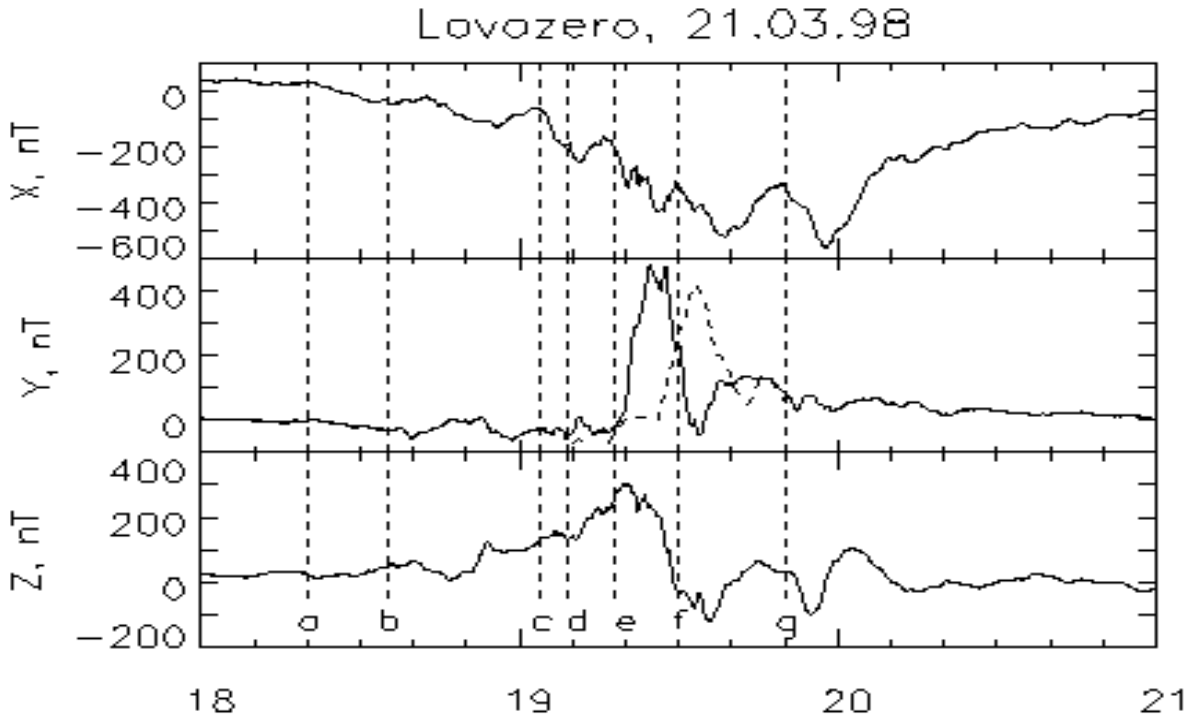

Fig. 1. Magnetic variations, Lovozero. Y-component of the Kiruna magnetometer is shown by the broken line. Vertical lines indicate moments of substorm dynamics mentioned in the text.

available has been chosen for this case study. Even so, we found several substorm intensifications within this short simple disturbance. It became evident, that the temporal fragmentation of the substorm active phase into several intensification steps and spatial fragmentation of the nightside oval into local sectors with different type of the activity is the main feature of the magnetospheric substorms.

EXPERIMENTAL DATA

Figure 1 presents ground-based magnetometer records from the Lovozero and Kiruna Observatories. Solar wind parameters were measured by IMP 8 situated at GSM (X, Y, Z) = (1.6×10^5, 7.35×10^4, 9.8×10^4) km. As shown in Figure 2, the IMF was southward for 100 minutes prior to a northward turning that corresponds to the substorm onset. The LANL geosynchronous spacecraft provide energetic particle observations that can be used to indicate magnetospheric substorm phases. Deep decreases of the particle flux, so-called flux-dropouts, occur during the substorm growth phase (Sauvaud and Winckler, 1980) while particle flux recovery from the dropout begins simultaneously with substorm onset. At substorm onset similar temporal structure also exhibit dispersionless injections, but the increase particle intensity is much higher and the origin is different. While injections result from in-situ particle acceleration within the trapping region, recoveries from dropouts result from reentries into the trapping region during magnetic field dipolarizations. The particle increase observed by LANL -97A at 1919 UT is an injection event, but all the other particle flux increases shown in Figures 3 and 8 are dropout recoveries.

POLAR provides auroral oval UV images from its high altitude ecliptic orbit each 1 to 3 minutes. We have used them to

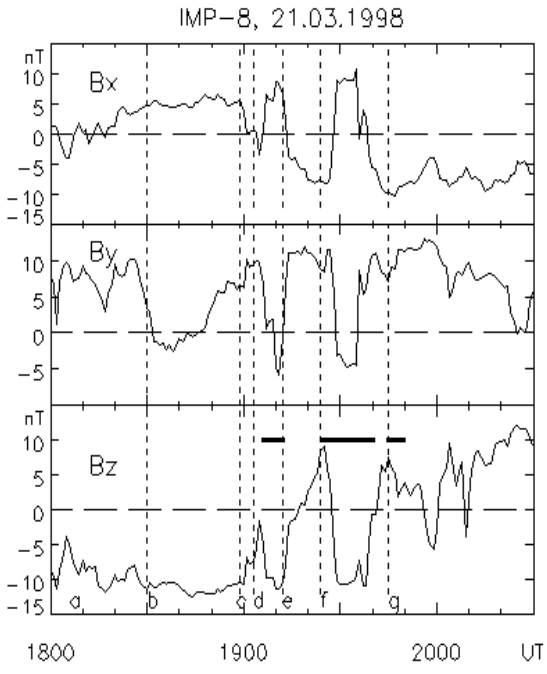

Fig. 2. IMP 8 interplanetary magnetic field data.

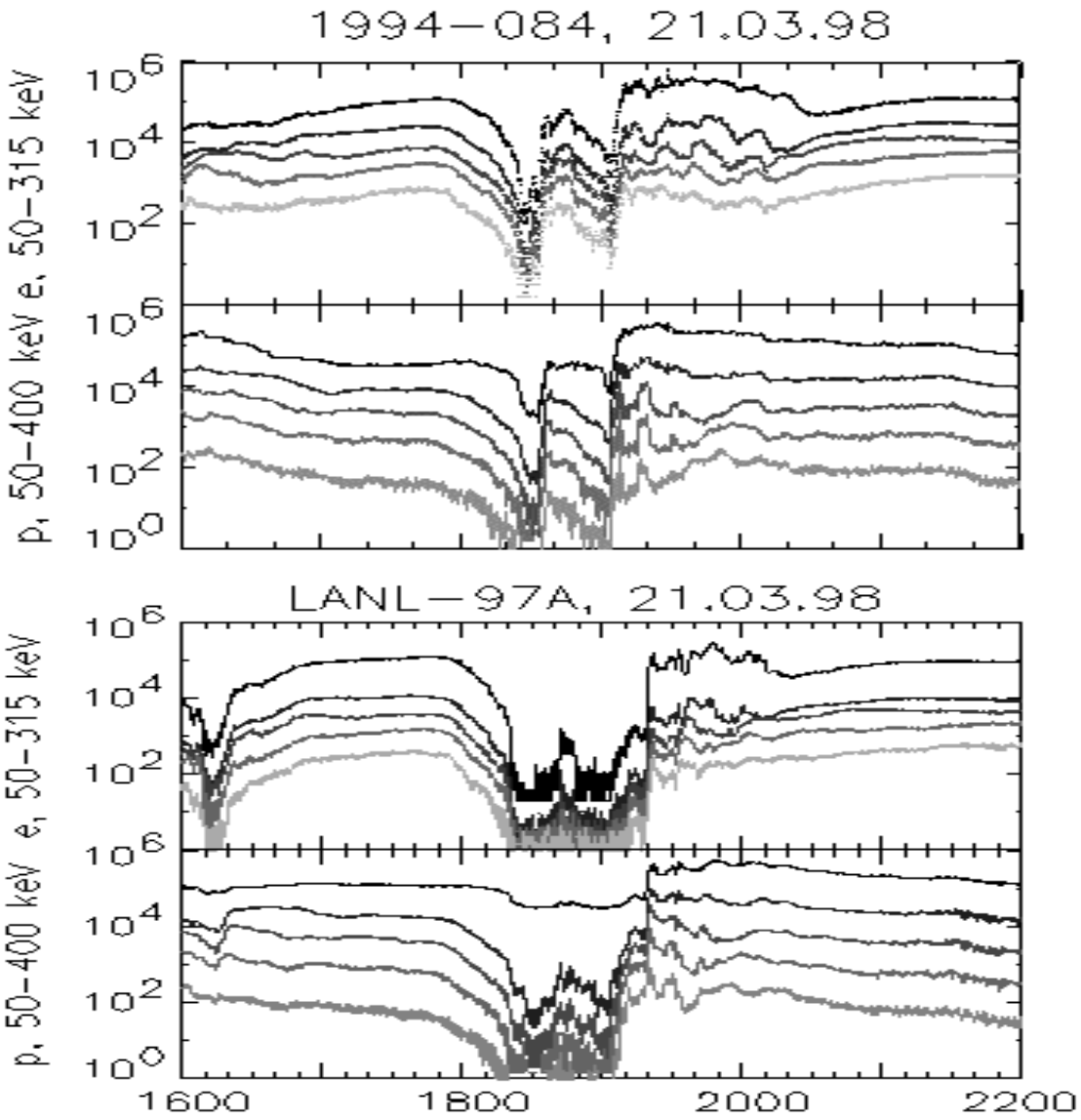

Fig. 3. Energetic electron and proton intensity measured by the LANL geostationary satellites: LANL-97A(69.8° E) and 1994-084 (103.5° E).

describe the global substorm development. We will repeatedly refer in the text to POLAR UV images, but lack of space forces to show the bulge scheme in Figure 4.

Ground-based auroral data were obtained from the Lovozero Observatory TV camera with an all-sky optical lens. The records were digitised to produce the north/south keogram shown in Figure 5. It presents the auroral luminosity profiles along the Lovozero central meridian. Figure 6 presents selected TV frames.

The spatial structure and temporal development of the energetic electron precipitation were available from the POLAR/ PIXIE instrument which observed the albedo of bremstrahlung X-rays (Imhof et al.,1995). We show the integrated flux variations in Figure 7, although pictures of the global auroral X-ray oval are available with 5 minute resolution.

SUBSTORM DEVELOPMENT

The H-component of the Apatity magnetogram indicates that the substorm developed as a negative bay with several intensifications. The vertical dashed lines mark the substorm timing: *a*) the start of the growth phase, *b*) the «pseudobreakup» intensification, *c*) the first onset activation, d) the beginning of the bulge expansion, *e*) and *f*) the first and the second WTS intensifications, and *g*) the last local intensification. We will describe the substorm development phase by phase including short discussion into each section.

Growth Phase and the Pseudobreakup

The growth phase was obscure. When a weak auroral arc became visible in the POLAR UVI images at 1820 to 1830 UT, some 30-40 min before the onset, it was located at 65° N, south of the Kola Peninsula (not shown). Auroral arcs occur at these latitudes only during strong substorms. We suggest that this can be explained by the influence of the quasi-trapped particles remaining from the previous activity (AL was equal to 1400 nT at 1600 UT). The Lovozero magnetometer recorded the gradual beginning of the negative bay in the H-component as a typical growth phase signature at 1820 UT (Figure 1). The Bz component of the IMF (Figure 2) turned southward at 1720 UT, 100 minutes before the beginning of the substorm active phase. The flux dropout which LANL spacecraft 1994-084 (at 103.5°E) and LANL-97A (at 69.8°E) began to observe at 1800 UT indicates the start of an enhanced growth phase (Figure 3). By 1830 UT both spacecraft observed a deep dropout, demonstrating that field lines became more tail-like and that the trapping boundary had shifted earthward in the midnight and the morning sectors.

POLAR UVI observations indicate that the first spontaneous intensification took place from 1830 to 1840 UT in the middle of the growth phase. The particle flux at spacecraft 1994-084, located in the same sector, recovered rapidly at 1835 UT. LANL-97A, located westward of the active region, recorded a smaller and shorter particle flux increase. As shown by Sauvaud and Winckler, (1980), recoveries from dropouts coincide with substorm onsets, but in our case this pseudobreakup was short (<5 min), localised, and exhibited almost no poleward expansion, so it cannot be classified as a substorm. The fact, that such events correspond to the fast tailward shifts of the trapping boundary, suggests that we must consider the onset process and the poleward expansion separately . It seems that the onset instability and magnetic field dipolarizations are more frequent and observed at breakups, pseudobreakups and other substorm intensifications, while the development of poleward expansions demands some special conditions.

Substorm Onset and Auroral Bulge Poleward Expansion

Figure 4 presents schematically the active phase dynamics as seen by the POLAR UVI. The onset occurs in two steps: from 1905 to 1906 UT the equatorward arc brightens (*c*), and later the poleward expanding auroral bulge forms between 1907 and 1909 UT (*d*). The first type of onset, the azimuthally extended auroral activation (AAF) was described by Elphinstone et al, (1995): auroral activations began in several spots on the arc, and later one of the spots developed into the auroral bulge. We can add now to this scheme that the bulge development suppress AAF on its flanks. The center of the bulge was located over Siberia, the western boundary remained fixed eastward of Kola Peninsula during the expansion until the WTS explosions at 1918 UT and 1930 UT (*e* and *f*). The eastern boundary of the luminosity gradually expands toward the morning sector as usual, due to the electron drift.

After a short particle flux recovery caused by the pseudobreakup at 1830 UT, both LANL spacecraft reentered a deep dropout, demonstrating that the trapping boundary had shifted earthward in the midnight and morning sectors. The beginning of the particle flux recovery from this dropout at both spacecraft coincide with a substorm onset (the equatorial arc brightening) and was finished well before the end of the auroral expansion. LANL 1994-084, which was in the morning sector at 103.5°E, observed a full particle flux recovery at 1910 UT at the beginning of the bulge formation, whereas the particle flux recovery on LANL-97AA (69.8°E) was only partial.

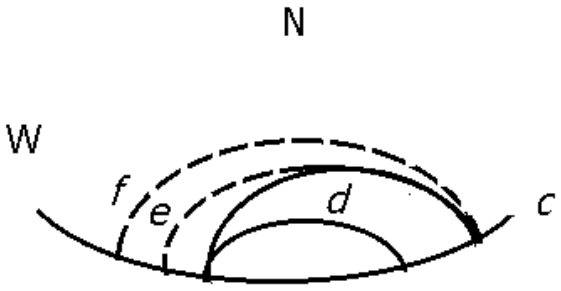

Fig. 4. Scetch of the auroral oval dynamics as seenby POLAR UVI

Local Growth Phase

As seen on the Lovozero keogram from 1912 to 1918 UT, the latitudinal width of the auroral oval east of the bulge (sometimes is referred to as the horn) decreased, and auroral forms moved southward similar to the auroral dynamics during substorm growth phase caused by the enhanced convection. We term this effect the «local growth phase» (LGP) since it coincides with an auroral bulge expansion in the adjoined local sector. In agreement with the auroral LGP signature, the energetic particle detectors of the LANL spacecraft closest to the Kola Peninsula (LANL-97A) observed an energetic electron and ion flux recovery come to a standstill at 1912 UT and an electron flux decrease begin at 1915 to 1918 UT (Figure 3). Therefore shortly after a simultaneous magnetic field dipolarization and auroral bulge expansion in one local sector, a LGP and magnetic field stretching into a tail-like configuration were registered to the west.

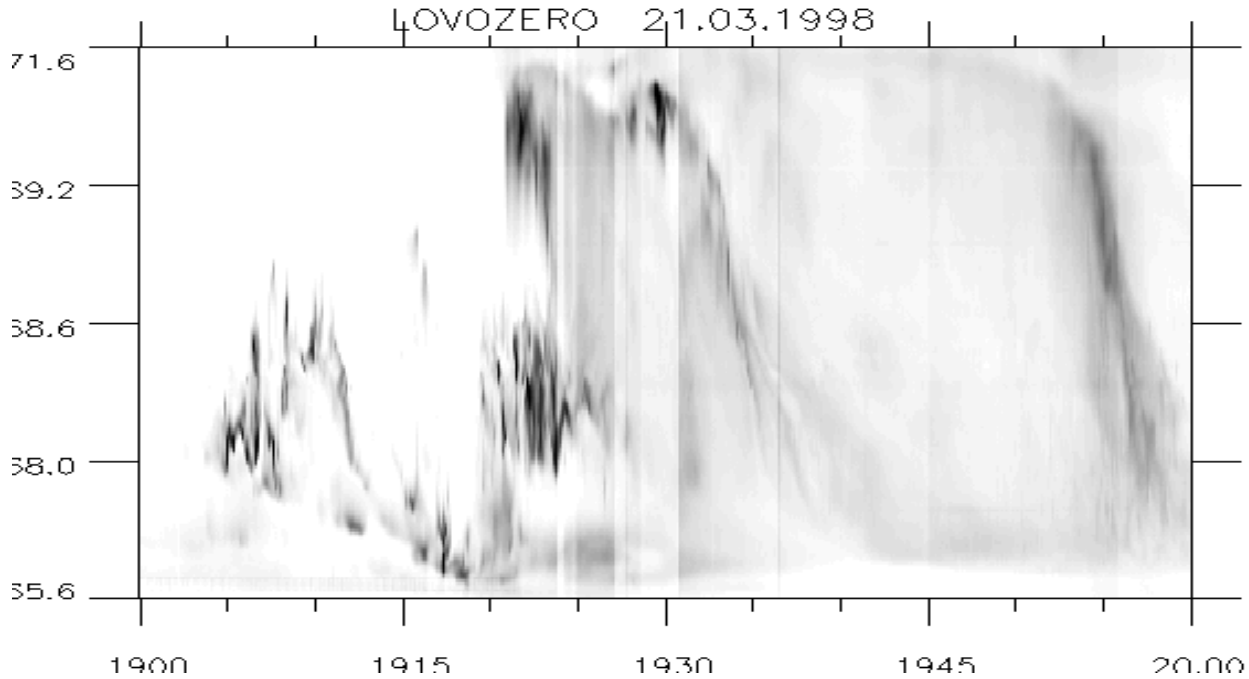

Fig. 5. The N-S keogram based on Lovozero auroral TV observations, 1900-2000UT /negative/.

Similar situations occurred over the Kola peninsula at 1935 UT and 1950 UT. An auroral intensification in one sector and the LGP type of equatorward shift of the auroral forms in another were recorded. The keogram shows features typical for the growth phase auroral displacements, while the global POLAR UVI frames (not shown) revealed an active aurora in the flank region.

An explanation for such fragmentation of the substorm activity lies in the restructuring of the convective electric field. Maynard et al. (1998) reported that spacecraft located near the center of the substorm onset observe dusk to dawn (revered) electric fields. These change the global electric field distribution, increasing electric field strengths in adjacent regions and enhancing the local growth phase. In turn, the LGP prepares conditions for a new intensification that may be either spontaneous or triggered.

Westward Travelling Surge and N-S Electrojet

The second substorm intensification prepared by the LGP was of the WTS type, which covered the Kola Peninsula from 1917 to 1920 UT. The auroral keogram shows (Figure 5), that the active aurora settled down on three latitudinal levels - closer to the pole, at the zenith, and in the south. The poleward aurora approached from the east, whereas the activity in the central area came from the west, where at 1918 UT POLAR UVI registered a spot of auroral intensification. The dynamic twirled structure created by the countermoving flows may result from (or display) a strong longitudinal current wedge. Figure 6 shows selected frames for the WTS development. The abrupt border of the WTS is an area of increased electron precipitation that creates a north/south ionospheric current, as indicated by a sharp burst in the Y - component of the magnetic disturbance**(** Figure 1**).**

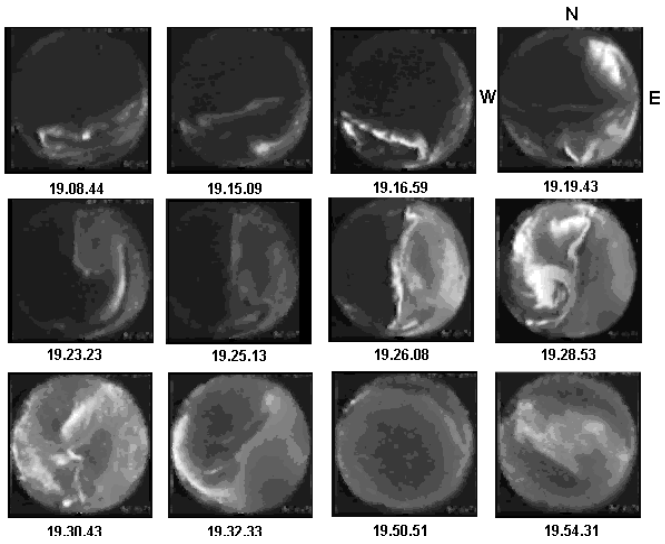

Fig. 6. Selected auroral TV frames , Lovozero. The sensitivity of the TV camera was changed by the operator at 1923 and 1926 UT.

The second jump of the WTS to Scandinavia occurred at 1930 UT, when the north/south electrojet deviation repeated over the Scandinavian stations. The Lovozero keogram showed a simultaneous displacement of the northern group of arcs to the south which may be classified as a new local growth phase. The polar part of the double oval remained unaffected by this process, which means that the LGP occur within the trapping region of the magnetosphere.

Energetic Particles, Pixie/POLAR and LANL Satellites

The PIXIE detector on POLAR recorded an X-ray oval during this event. Figure 7 presents the integrated X-ray flux at several local time sectors. The acceleration of the energetic electrons began at the 1904 UT substorm onset (24-03 LT) and it is possible to see that all substorm intensifications were accompanied by the X-ray enhancements in the associated local sectors. The bottom section of the Figure 8 shows the integrated X-rays flux over the Lovozero TV camera field of view. The flux increase between 1915 and 1920 UT coincided with a local WTS intensification over the Kola Peninsula. The accelerated high energy particles indicate that the WTS did not merely continue the onset, but rather represented a new instability.

The particle flux recovery from the dropout on LANL-97A associated with WTS began at 1918:40 UT; the first 40s step was synchronous for all energies and particle species. An inspection of the Lovozero TV data shows that the eastern edge of the sky slowly began to brighten about 1917 UT and the first bright spot there emerged at 1918:40-1918:50 UT. Therefore within an accuracy of 10s the response of the trapping boundary to the WTS onset was simultaneous. The dropout recovery was dispersionless for the electrons and coincided with the WTS development over the Kola Peninsula. The proton increase was energy-dependent, shorter for the high energy particles. The particle flux increased due to the trapping boundary motion, possibly with some additional acceleration, but it was not a real injection event in which the particle intensity increased by one or two orders of magnitude above normal radiation belt levels. The trapping boundary expanded and the satellite found itself on the slope of the radiation belt but still not deep enough for the encounter with the expanding auroral bulge magnetic tubes which ought to be populated by freshly injected energetic particles.

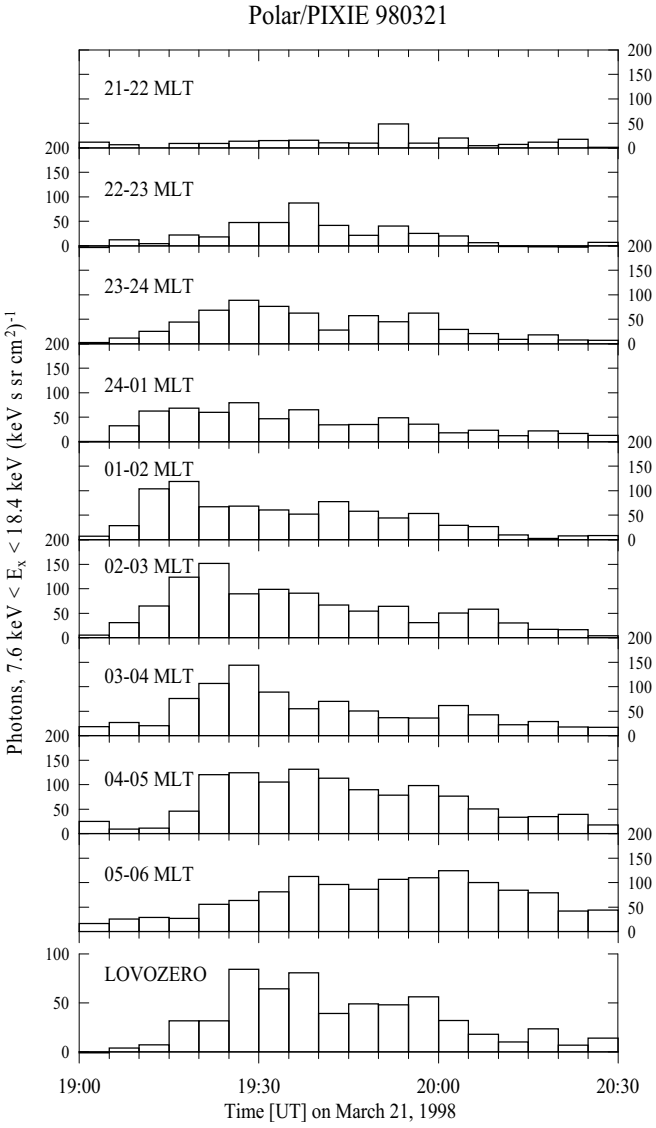

Fig. 7. Polar/PIXIE, 7.57keV < Ex < 18.4keV. Integrated flux in several local time sectors and over Lovozero TV field of view.

Solar Wind Magnetic Field and Triggering Effect

IMP 8 was situated at GSM (X, Y, Z) = (1.6×10^5, 7.35×10^4, 9.8×10^4) km. The solar wind velocity increased from 420 to 520 km s^{-1} from 1800 to 2000 UT. Simples estimations for the lag times needed for the solar wind to reach the subsolar magnetopause at X = 10 R_E and the nightside trapping boundary at X = -10 R_E give 3.1 and 5.8 min, respectively. The dotted lines in Figure 2 indicate the moments of the substorm intensification with a 5 min shift to account for this delay. One can see that not only the substorm onset, but also two out of the three following substorm intensifications could be associated with the certain steps of the pulsating northward IMF turnings. The solid horizontal bars show the times of LGPs with the same lags. The first two LGP coincide with negative Bz turnings and the third with a drop in Bz, indicating that the LGP depends not only on the simultaneous auroral bulge activation, but also requires enhanced convection.

CONCLUSION

The substorm of March 21, 1998 exhibited most of the features of a classical substorm (Akasofu, 1968), and the main auroral substorm modules described by Elphinstone et al, (1996), including a pseudobreakup during the growth phase, a brightening of the equatorial arc, an auroral bulge with the poleward expansion, and the WTS-type intensifications. A close relationship to solar wind parameters was found not only at substorm onset but also during the following intensifications. Some were presumably triggered by the IMF Bz variations, although at least one intensification was spontaneous.

We found that the global growth phase was transformed after the onset into the local growth phase in the restricted sector, when an auroral bulge expansion was observed in the adjacent region. We can describe the relationship between the global and the local substorm processes as a fragmentation of the night side auroral magnetosphere into two or more sectors. The traces of this process were observed not only in the active auroras, but also in the dynamics of the trapping boundary. The auroral bulge expansion might be considered to be the main driving force of the fragmentation: by decreasing or reversing the convective electric field in a bulge region it enhances convection in the adjoining regions. In turn, the local growth phase prepares a favourable conditions for the next intensification in this region. As a result a spatial fragmentation causes temporal fragmentation of the substorm active phase into several intensification. That can explain why it is so difficult to found classical isolated substorm with single onset and poleward expansion.

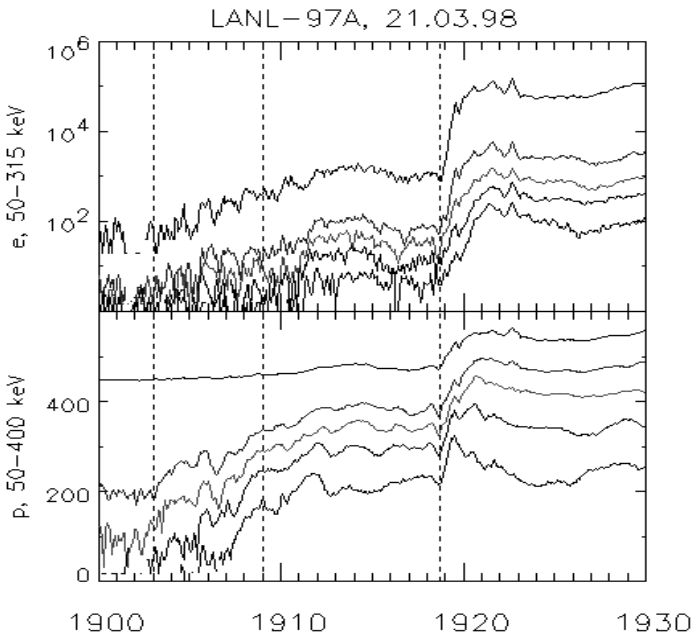

Fig. 8. Details of the dropout recovery, LANL-97A

The behaviour of the energetic particles near the trapping boundary indicates that the particle injections which are usually collocated with the active auroral intensifications take place inside of the boundary. Therefore the magnetic field lines from the latitudes of the northern edge of the bulge (75°N) must project to the equatorial magnetosphere earthward from the geostationary region. That demands considerable revision of the accepted image of the night-side substorm magnetic field configuration. While in general it is possible to understand the features described above within the framework of the inner magnetosphere substorm models. (Lui, 1991; Roux et al., 1991).

REFERENCEES

Akasofu, S.-I., Polar and magnetospheric substorms, D.Reidel Oub. Co.,Dordrecht-Holland, 1968.

Elphinstone, R. D., Observations in the vicinity of substorm onset: Implications for the substorm process, *J. Geophys. Res.,* 100, 7937-7969, 1995.

Elphinstone, R. D., J. S. Murphree, and L. L. Cogger, What is a global auroral substorm?, *Rev. Geophys*., **34**, 169-232, 1996.

Imhof W.L., Spear K.A., Hanultor J.W. et al., The polar ionospheric X-ray imaging experiment (PIXIE) *Space Sci. Rev*. 1995. V. 71. P. 385.

Lui, A. T. Y., A synthesis of magnetospheric substorm models*, J. Geophys*. Res., 96, 1849-1856, 1991.

Maynard N. C., G.M. Erickson, W.J. Burke, and G.R. Wilson, Magnetospheric electric fields during substorm onset and expansion phases, in: Substorm-4, Edd. by S. Kokubun and Y. Kamide, Terra Sci., 605-610, 1998.

Rostoker, G., S.-I. Akasofu, J. C. Foster, R. A. Greenwald, Y. Kamide, K. Kawasaki, A. T. Y. Lui, R.L. McPherron, and C. T. Russell, Magnetospheric substorms-definition and signatures, *J. Geophys. Res*., **85**, 1663-1668, 1980.

Roux, A., P. Perreault, P. Robert, A. Morane, A. Pedersen, et al., Plasma sheet instability related to the westward travelling surge, *J. Geophys. Res*., 96, 17697-17707, 1991.

Sauvaud, J. A. and J. R. Winckler, Dynamics of plasma, energetic particles and fields near synchronous orbitin the nighttime sector during magnetospheric substorms, J. *Geophys. Res*., **85**, 2043-2056, 1980.

Sharma A. S., and Baker D. N., What triggers substorm expansion onset? Current understanding and outook, Substorms-4, ed. by S. Kokubun and Y. Kamide, pp. 245-248, Terra, Tokyo, 1998.

Reported at COSPAR 33, Warshawa, 2000; Accepted by Adv. of Space Sci.